1 INTRODUCTION

Investigation into the field of lepton-pair production in hadronic interactions began with an experiment carried out at Brookhaven National Laboratory in 1970 [Chr 70]. This experiment studied the reaction $p\mathrm{U} \to \mu^+\mu^- X$ for proton energies between 22 and 29 GeV, resulting in pair masses between 1 and 6.7 GeV[1]. The data above ~ 3 GeV (where the J/ψ resonance family would later be found) exhibited a rapidly decreasing continuum of muon pairs. The steeply falling nature of the cross section was explained later that year by Drell and Yan [Dre 70], who were interested in dilepton production as a possible application of the quark-parton model of hadron structure outside of deeply-inelastic scattering experiments. Their model of quark-antiquark annihilation through the electromagnetic interaction, which has become known as the Drell-Yan process, was generally successful in describing the data and would only improve as our understanding of the strong interaction improved.

The Drell-Yan process still remains an active area of experimental and theoretical research some thirty years later. It has played a key role in developing the mathematical technology of perturbative Quantum Chromodynamics (QCD), being one of the first processes to be calculated to next-to-leading order $\mathcal{O}(\alpha_s)$, and remains one of the few processes to be calculated to next-to-next-to-leading

[1] Throughout this thesis, we will utilize "God-given" units, setting $\hbar = c = 1$.

$\mathcal{O}(\alpha_s^2)$. Experimentally it has provided a wealth of information about nucleon structure; its confirmation of the quark-parton model and its verification of the quark charge assignments being two notable early applications. In this thesis we describe and report the results of an absolute measurement of the dimuon cross sections from the interaction of an 800-GeV proton beam with hydrogen and deuterium targets. As will be shown, these data provide important information about the distributions of antiquarks in the nucleon sea.

1.1 Background

The disciplines of high-energy and particle physics consist of the search for the ultimate constituents of matter and the study of the fundamental interactions between them. With the introduction of Quantum Chromodynamics in the mid-1970's, a consistent treatment of the weak, electromagnetic and strong interactions was finally realized. The gauge field theories of Quantum Electrodynamics (QED) and the Weinberg-Glashow-Salam model had long treated the electromagnetic and weak interactions felt by the leptons – the electron (e), muon (μ), tau (τ), and associated neutrinos (ν_e, ν_μ, ν_τ) – as the exchange of gauge field bosons (the photon (γ) and the $W^\pm$ and Z^0 bosons). Attempts to formulate similar theories for the strongly interacting hadrons, however, initially met with only limited success. The realization by Gell-Mann and (independently) Zweig in 1964 that the hadron spectrum could be explained in terms of three fractionally charged

Table 1.1: Properties of the light quarks. Shown are the isospin (I) and its third component (I_3), strangeness (S), baryon number (B) and charge (Q/e).

flavor	I	I_3	S	B	Q/e
u	1/2	1/2	0	1/3	2/3
d	1/2	$-1/2$	0	1/3	$-1/3$
s	0	0	-1	1/3	$-1/3$

fermionic constituents, called quarks, set the stage for the development of QCD and its inclusion in what has become known as the Standard Model.

Although Gell-Mann and Zweig's static quark model needed only three different quark flavors, experiment confirms the existence of six, with larger numbers being ruled out in the framework of the Standard Model by recent experiments. The six quarks are conventionally known as up (u), down (d), strange (s), charm (c), bottom (b) and top (t) and are found only in bound states called hadrons: mesons ($\pi^{\pm}$, π^0, J/ψ, etc...) are quark-antiquark ($q\bar{q}$) bound states, while baryons (p, n, Δ^{++}, etc...) are the bound states of three quarks (qqq). Table 1.1 shows the quantum numbers of the three quarks of the first three quarks. In order to avoid violating the Pauli principle in baryons such as the Δ^{++} (uuu), the static quark model had to add an additional quantum number called color. Each quark carries one of three colors (red, green or blue). An object in which all three colors (or one color and its anti-color) are present is a color-neutral (color-singlet) state.

Color was an *ad hoc* addition to the static quark model. The role which it plays in QCD is more fundamental. QCD is a non-Abelian color gauge field theory, the three colors representing the fundamental basis of the $SU(3)$ symmetry group. Color plays essentially the same role in the strong interaction as electric charge in electromagnetism, the principal difference being the number of "charge" states – two electric charge states (+ and −) versus six color states (r, g, b, $\bar{r}$, $\bar{g}$, $\bar{b}$)[2]. The quarks interact through the exchange of QCD's gauge field bosons, the gluons (g). Unlike the photons in QED, which are electrically neutral, the gluons carry color charge. This leads to some important differences. A well-known property of QED is the running of the electromagnetic coupling constant $\alpha \approx \frac{1}{137}$. A test charge polarizes the virtual e^+e^- pairs surrounding it, leading to screening of the test charge at larger distances, resulting in an effective reduction in α. Probing the test charge at smaller distance scales, i.e. larger momentum transfers (q^2), results in an observed increase in the coupling. The same effect occurs in QCD, but the color-charged gluons are self interacting. This leads to an antiscreening of the color test charge, resulting in a decrease in the strong coupling constant (α_s) with increasing q^2. This property of the strong interaction is known as asymptotic freedom.

Owing to the mathematical complexity of the $SU(3) \otimes SU(2) \otimes U(1)$ Standard Model, exact solutions are often not possible for physical interactions. We must

[2]Red, green, blue and their anti-colors.

therefore rely upon perturbation theory to obtain meaningful predictions from the model. This has never presented a problem in either the weak or electromagnetic interactions, where one can simply carry out the perturbative expansion in the coupling constant to whatever level of precision is desired. However, the strong interaction derives its name from the fact that it is a *strong* interaction. For momentum scales on the order of the proton mass, the size of the strong coupling constant ($\alpha_s(M_p^2) \sim 1$) renders fixed-order perturbation theory meaningless – all orders in the perturbative expansion are significant. Fortunately, the asymptotic freedom exhibited by QCD results in a strong coupling constant which decreases with increasing q^2. At momentum-transfers typical of high-energy fixed-target experiments, α_s becomes sufficiently small that it may be reliably used as an expansion parameter. Nevertheless, it remains sufficiently large that terms next-to-leading order in α_s may remain important.

An additional complication in hadronic interactions is that we cannot be certain which of the interacting partons (the quark, antiquark and gluon constituents) are participating in the interaction. We can at best speak of the probability of finding a given parton carrying a fraction x (called Björken-x) of the interacting hadron's momentum, which we in general denote by $f_{q/A}(x)$ for a parton of type q in a hadron of type A. Calculations of physical processes in the Standard Model are thus predicated on prior knowledge of these parton distribution functions (PDF's).

Of particular importance to many experiments are the parton distributions in the nucleon (i.e. $u(x) = f_{u/p}(x)$, $\bar{u}(x) = f_{\bar{u}/p}(x)$, etc...). Early parameterizations of the PDF's relied on fits to the structure functions measured in deeply-inelastic lepton-hadron scattering experiments (DIS), which are primarily sensitive to the light quark distributions ($u(x)$ and $d(x)$). More modern parameterizations, such as those performed by the CTEQ, MRST and GRV collaborations [MRST, CTEQ, GRV] use several different physical processes to extract complementary information about the parton distributions. The lepton-charge asymmetry observed in $W^{\pm}$ production provides additional information about the light quark distributions, while jet production and prompt photon measurements are used to constrain the gluon distributions. The Drell-Yan process for dilepton production, which involves quark-antiquark annihilation, provides constraints on the light antiquark distributions ($\bar{u}(x)$ and $\bar{d}(x)$) in the nucleon sea. The CTEQ 5 set of parton distributions is shown in figure 1.1, along with the light antiquark distributions from the MRST 98 and GRV 98 distributions.

1.2 The Drell-Yan Process

Prior to the introduction of QCD, hadronic interactions were calculated with some success using the quark-parton model, whereby the interacting partons (quarks and antiquarks) were treated as being free of the strong interactions on the timescale of a hard interaction (the impulse approximation). Cross sections

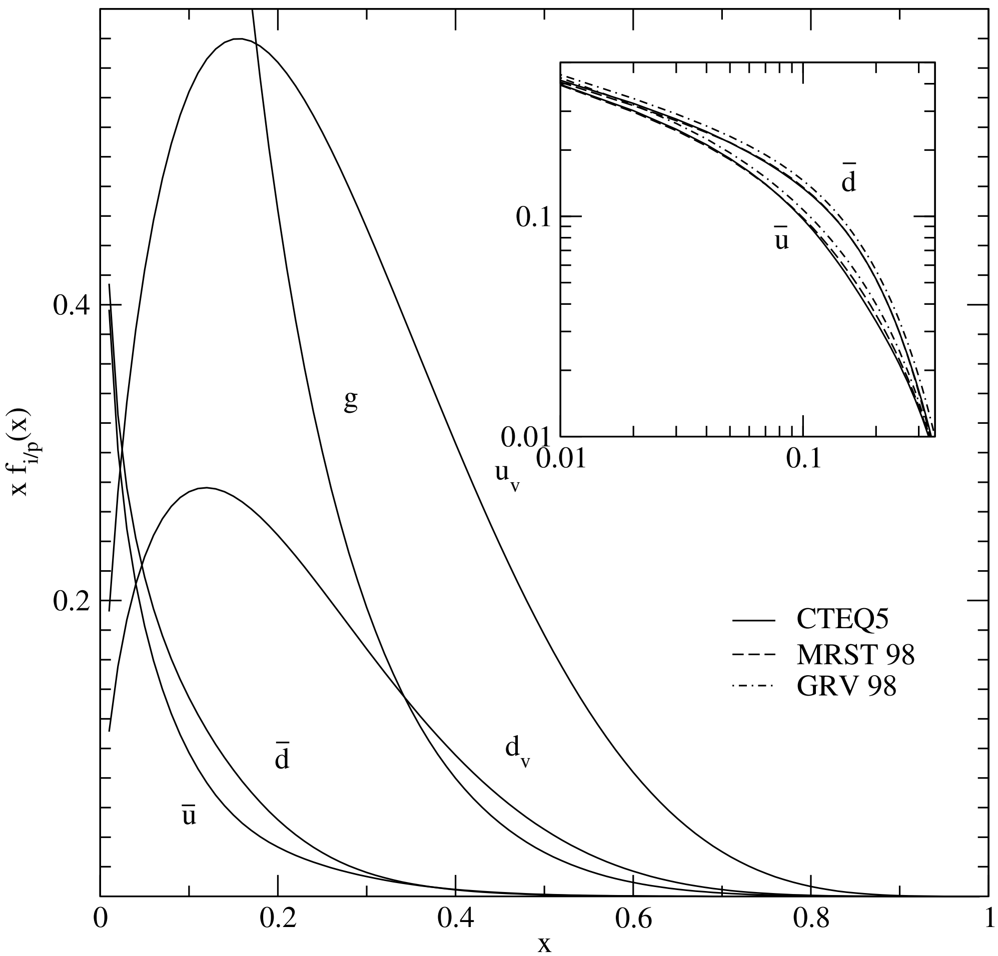

Figure 1.1: CTEQ5 partons. Shown are the valence quark and light anti-quark distributions, and the gluons. The inset compares $\bar{d}(x)$ and $\bar{u}(x)$ from the CTEQ5 [CTEQ], MRST 98 [MRST] and GRV 98 [GRV] fits.

involving hadrons were then reduced to the comparatively simple problem of calculating the parton-level cross sections and folding in the probability to find the particular parton configuration. Figure 1.2 shows the Feynman diagram for the Drell-Yan process for lepton pair production in proton-nucleon collisions in the dimuon channel studied by E866. In the initial state, a quark (antiquark) carrying a fraction x_1 of the beam's momentum annihilates an antiquark (quark) carrying a fraction x_2 of the target's momentum. This results in a time-like ($q^2 > 0$) intermediate photon, which decays into the final state $\mu^+\mu^-$ pair.

1.2.1 Kinematics

In the lab, we measure the invariant mass of the muon pair, and their total longitudinal momentum. The mass of the dimuon is related to the momentum fractions of the interacting partons by

$$q^2 = M^2 = s\,x_1 x_2 \tag{1.1}$$

where s is the total four-momentum squared of the interacting hadrons. The longitudinal momentum of the dimuon, as a fraction of its maximum possible value ($p_L^{\max} \approx \sqrt{s}/2$), is referred to as Feynman-x (x_F). It is related to the initial state momentum fractions by

$$x_F = \frac{p_L}{p_L^{\max}} = x_1 - x_2. \tag{1.2}$$

Thus, measurement of the invariant mass and x_F of the muon pair allows us to determine the momentum fractions carried by the interacting partons. Solving for x_1 and x_2 in equations 1.1 and 1.2 we find

$$x_{1,2} = \frac{1}{2}(x_F \pm \sqrt{x_F^2 + 4\tau}) \tag{1.3}$$

where we have taken $\tau = x_1 x_2 = M^2/s$.

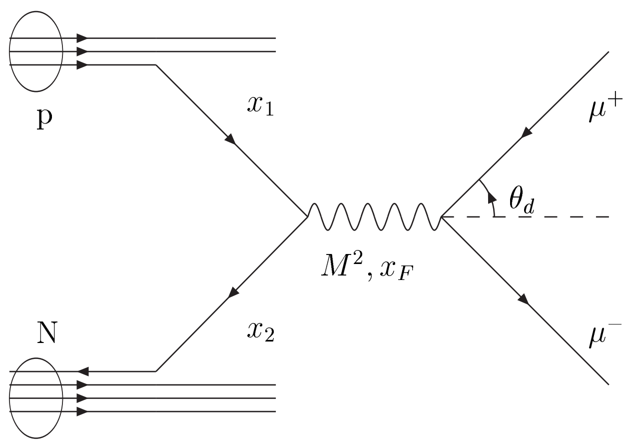

Figure 1.2: The Drell-Yan process for dimuon production.

In order to completely specify the the final state of the interaction, we need four more variables. One of these is the momentum of the muon pair transverse to the beam, denoted by p_T. This is expected to be small in the Drell-Yan process: $< p_T > \approx 0.3$ GeV, non-zero only due to Fermi smearing of the momenta of the interacting partons. The larger values of p_T which are observed in dilepton production require additional partons in the final state, which are provided by the higher-order QCD processes which we discuss later.

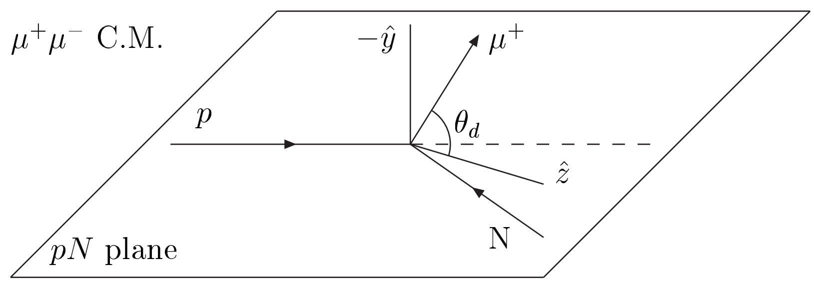

Figure 1.3: Definition of the Collin-Soper frame.

The three other variables which characterize the process are the polar decay angle θ_d, and the azimuthal production and decay angles ϕ_p and ϕ_d respectively. These variables are most naturally defined with respect to the $q\bar{q}$ annihilation axis. However, when p_T is non-zero, this axis becomes difficult to measure. The angular variables are therefore measured with respect to the Collins-Soper frame [Col 77], which is shown schematically in figure 1.3. In this frame, the z-axis is taken to be parallel to the bisector of the angle between the interacting hadrons in the rest frame of the virtual photon.

1.2.2 Cross Section

The cross section for the Drell-Yan process is easily constructed in the quark-parton model. The assumption that the interacting quark and antiquark are free on the timescale of the hard interaction allows us to factor the cross section into a short distance $q\bar{q}$ annihilation term ($\sigma_{q\bar{q}}$), and a term expressing the probability of finding the particular partonic configuration. The $q\bar{q}$ annihilation cross section is simply given by [Dre 70]

$$\sigma_{q\bar{q}} = \frac{1}{3}\frac{4\pi\alpha^2}{3M^2}e_q^2 \tag{1.4}$$

which is just the cross section for the annihilation of two fermions in QED, multiplied by a factor of 1/3 required by color conservation and a factor of e_q^2 to account for the fractional charge of the quarks. Multiplying by the probability of a quark (antiquark) in the beam annihilating an antiquark (quark) in the target and summing over all parton species we have an expression for the Drell-Yan cross section differential in x_1 and x_2

$$\frac{d^2\sigma_{AB}}{dx_1 dx_2} = \frac{1}{3}\frac{4\pi\alpha^2}{3M^2}\sum_{q\in u,d,s,\ldots} e_q^2 \left[f_{q/A}(x_1)f_{\bar{q}/B}(x_2) + f_{\bar{q}/A}(x_1)f_{q/B}(x_2)\right]. \tag{1.5}$$

Expressed in terms of quantities measured in the lab we obtain

$$M^2\frac{d^2\sigma_{AB}}{dM^2 dx_F} = \frac{1}{3}\frac{4\pi\alpha^2}{3M^2}\frac{x_1 x_2}{x_1+x_2}\sum_q e_q^2 \left[f_{q/A}(x_1)f_{\bar{q}/B}(x_2) + f_{\bar{q}/A}(x_1)f_{q/B}(x_2)\right] \tag{1.6}$$

where equation 1.3 is used to evaluate x_1 and x_2. Alternatively, we can express the cross section in terms of the dimensionless variables τ and $y = \frac{1}{2}\ln\frac{x_1}{x_2}$ (the rapidity)

$$s\frac{d^2\sigma_{AB}}{d\tau dy} = \frac{1}{3}\frac{4\pi\alpha^2}{3\tau}\sum_q e_q^2 \left(f_{q/A}(x_1)f_{\bar{q}/B}(x_2) + f_{\bar{q}/A}(x_1)f_{q/B}(x_2)\right). \tag{1.7}$$

This is known as the scaling form of the cross section.

1.2.3 Predictions

The Drell-Yan model makes some important predictions about the dilepton cross sections. The left-hand side of equation 1.7 is a function of the variables τ, y

and s, while the right-hand side is only a function of τ and y. Thus, the model predicts that the cross sections multiplied by s, and measured at different beam energies, but the same kinematics, should be the same – the cross sections should scale with $\frac{1}{s}$, and this is generally observed [Yoh 78, Con 89, Ant 82].

Another important prediction is the shape of the angular distributions. The angular distribution of the μ^+ in the pair rest frame can be expressed as [Cle 78]

$$\frac{d^2\sigma}{d\phi_d \, d\cos\theta_d} \propto 1 + \lambda \cos^2\theta_d + \mu \, \sin 2\theta_d \cos\phi_d + \nu/2 \sin^2\theta_d \, \cos 2\phi_d \tag{1.8}$$

where λ, μ and ν are functions of the other kinematic variables. For the Drell-Yan process, the assumption of massless quarks implies that the virtual photon is transversely polarized ($\lambda = 1$, $\mu = \nu = 0$), resulting in the prediction

$$\frac{d^2\sigma}{d\cos\theta_d} \propto 1 + \cos^2\theta_d \tag{1.9}$$

when θ_d is measured with respect to the $q\bar{q}$ annihilation axis. Several experiments [Con 89, McG 99, Cha 99, Bro 01] have confirmed that the dileptons are produced transversely polarized.

Despite these successes in describing experimental data, the Drell-Yan model also had some initial failures. Because there are no particles in the final state off which to recoil, any transverse momentum in the dilepton must originate with the initial state. The mechanism for this is most likely Fermi smearing of the parton distributions, and the expected size of this intrinsic k_T is small ($\sim$ 300 MeV). The observed (s-dependent) values of $< p_T^2 >\sim 1.75$ GeV^2 cannot be reproduced by this mechanism in the Drell-Yan process.

A second problem came about when absolute measurements of the dilepton cross sections were compared to Drell-Yan calculations based on the early PDF fits to DIS structure functions. Table 1.2 shows the K-factors, defined as the ratio of measured to calculated cross sections ($K = \sigma_{\mathrm{meas.}}/\sigma_{\mathrm{DY}}$), from several different experiments using different beams and targets. Typically, experiments measured a cross section which was a (nearly constant) factor of two larger than the Drell-Yan model and DIS structure function measurements implied. Along with the discrepancy in the p_T distribution, this was taken as a sign that QCD would play an important role in dilepton production.

1.3 QCD Modifications

With the introduction of QCD, the basic physics behind the Drell-Yan process was confirmed theoretically. That quark-antiquark annihilation gives rise to dilepton pairs is a consequence of the electromagnetic interaction. QCD provides substantial, albeit well-known, corrections to the leading-order (LO) electromagnetic contribution described by Drell and Yan. The diagrams which contribute at next-to-leading order (NLO or $\mathcal{O}(\alpha_s)$) are shown in figure 1.4. The gluon-bremsstrahlung and vertex-correction diagrams represent corrections to the basic $q\bar{q}$ annihilation picture of the Drell-Yan process, increasing the magnitude of the theoretical cross

Table 1.2: Experimental K-factors from several different early lepton pair production experiments.

Experiment	Interaction	Beam Momentum	$K = \sigma_{\text{meas.}}/\sigma_{\text{DY}}$
E288 [Kap 78]	$p\ Pt$	300/400 GeV	~ 1.7
WA39 [Cor 80]	$\pi^{\pm}\ W$	39.5 GeV	~ 2.5
E439 [Smi 81]	$p\ W$	400 GeV	1.6 ± 0.3
NA3 [Bad 83]	$(\bar{p}$ - $p)Pt$	150 GeV	2.3 ± 0.4
	$p\ Pt$	400 GeV	$3.1 \pm 0.5 \pm 0.3$
	$\pi^{\pm}\ Pt$	200 GeV	2.3 ± 0.5
	$\pi^{-}\ Pt$	150 GeV	2.49 ± 0.37
	$\pi^{-}\ Pt$	280 GeV	2.22 ± 0.33
NA10 [Bet 85]	$\pi^{-}\ W$	194 GeV	$\sim 2.77 \pm 0.12$
E326 [Gre 85]	$\pi^{-}\ W$	225 GeV	$2.70 \pm 0.08 \pm 0.40$
E537 [Ana 88]	$\bar{p}\ W$	125 GeV	$2.45 \pm 0.12 \pm 0.20$
E615 [Con 89]	$\pi^{-}\ W$	252 GeV	1.78 ± 0.06

section and providing a mechanism to reach larger values of p_T. Resummation techniques have been developed, which enable the calculation of such corrections to all orders in α_s. Taking K equal to the resummed cross section divided by the LO contribution gives $K \approx 1.8$ for α_s evaluated at q^2 typical of fixed-target experiments. This already accounts for much of the experimental K-factor.

The contributions described above are simply modifications to the basic $q\bar{q}$ picture of the Drell-Yan process – the main interaction is still the electromagnetic annihilation of the interacting partons, with the strong interaction only modifying the initial states of the $q\bar{q}$ pair. The gluon Compton-scattering diagram, however, is fundamentally different. Here, the incoming quark (antiquark) scatters off a gluon through the strong interaction, emitting the virtual photon which decays in the final state of the interaction. Theoretical studies of this process by Berger *et al.* [Ber 98] have shown that for transverse momenta large compared to the mass of the pair ($p_T > M/2$), the gluon Compton scattering diagrams dominate the cross section (accounting for $\approx 80\%$ of the NLO calculation). Therefore, with increasing p_T, the dilepton cross section becomes less sensitive to the antiquark distributions, and more sensitive to the gluons.

1.4 Motivation

The primary goal of Fermilab Experiment 866 (FNAL E866/NuSea) was to measure the ratio of continuum dimuon cross sections in proton-deuteron (σ_{pd}) interactions to those in proton-proton (σ_{pp}) interactions. These measurements are sensitive to the x-dependence of the ratio $\bar{d}/\bar{u}$ in the nucleon, and were motivated by several experiments [Ama 91, Bal 94, Ada 95] which demonstrated a large and previously unanticipated flavor asymmetry $\bar{d}/\bar{u} > 1$. The E866 results [Haw 98, Tow 01], which were based on a large sample of dimuon events

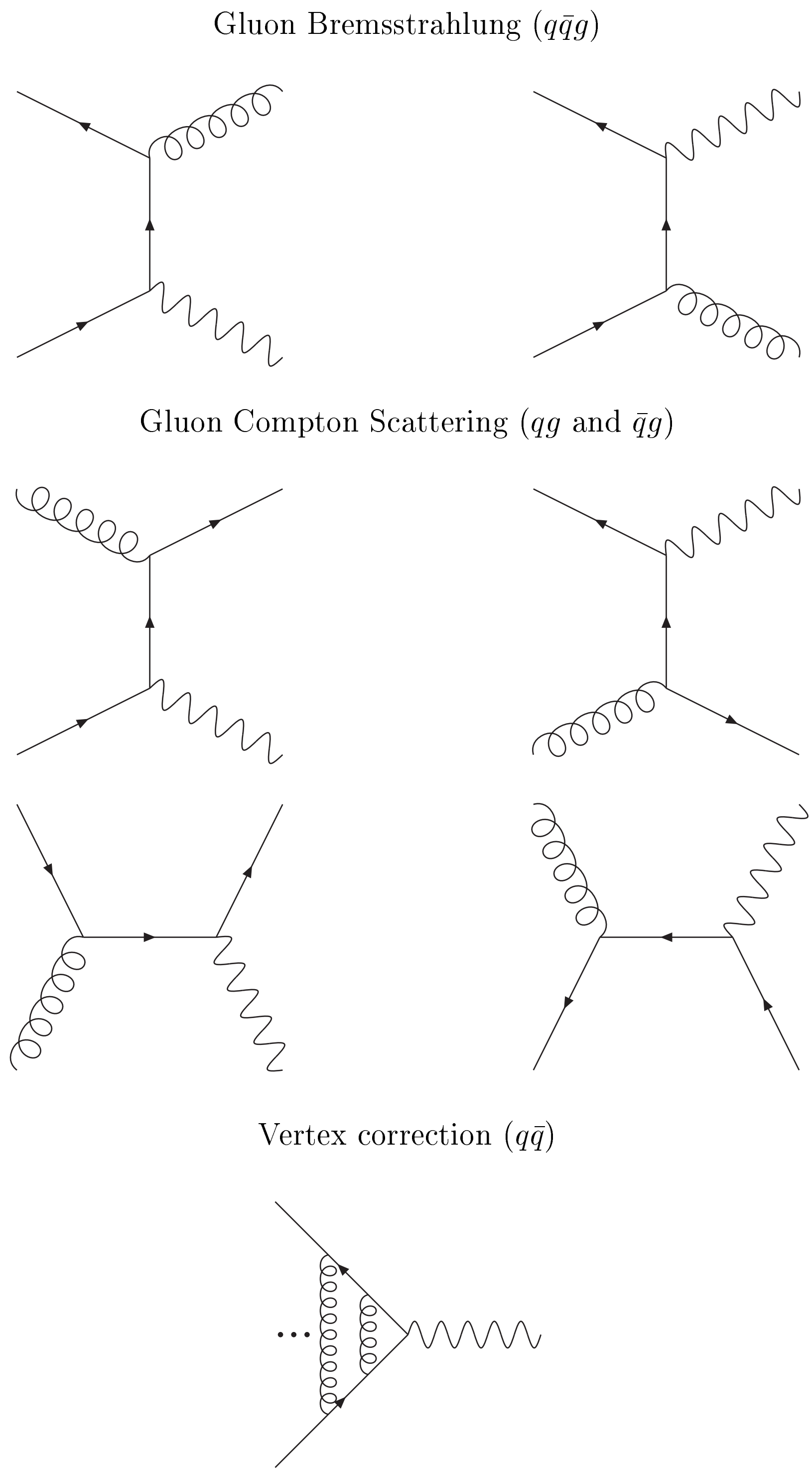

Figure 1.4: Next-to-leading order (NLO) diagrams which contribute to the dilepton cross section. The final state muon pair is omitted.

($\approx 360,000$) induced by an 800-GeV proton beam ($\sqrt{s} = 38.8$ GeV) interacting with hydrogen and deuterium targets, provided the first determination of the strong x-dependence of this flavor asymmetry.

Absolute measurements of the hydrogen and deuterium cross sections, the topic of this thesis, provide additional information on the magnitude and absolute shape of the light antiquarks. This can be easily shown by writing the leading-order cross section expression in equation 1.6 for various targets. Evaluating the sum for the hydrogen cross section, and taking the limit of large x_F appropriate for much of the E866 data[3] we have

$$\left(M^2 \frac{d^2\sigma}{dM^2 dx_F}\right)_{x_1 \gg x_2} \approx \frac{1}{3}\frac{4\pi\alpha^2}{3M^2}\left(\frac{4}{9}u(x_1)\bar{u}(x_2) + \frac{1}{9}d(x_1)\bar{d}(x_2)\right). \tag{1.10}$$

Owing to the larger charge-squared factor in front of the $u\bar{u}$ term and the size of the up distribution compared to that of the down distribution in the proton, about 80% of the proton cross section at leading order is due to the $u\bar{u}$ annihilation. Thus, to the extent that the valence distributions are known (DIS measurements constrain these well in our kinematic range), the proton cross section provides a direct measurement of the $\bar{u}(x)$ distribution.

The deuterium cross section can be similarly written. Nuclear effects in deuterium are small, and confined to small x_2 [Ald 90]. This allows us to express the deuterium cross section as the sum $\sigma_{pd} = \sigma_{pp} + \sigma_{pn}$. If we assume that charge

[3] In the large x_F limit, x_1 is sufficiently large compared to x_2 that we can neglect terms in the cross section with the antiquark in the beam and the quark in the target.

symmetry holds, then the parton distributions in the proton and neutron are related through $u(x) = d^n(x)$, $\bar{u}(x) = \bar{d}^n(x)$, etc.... This yields an expression for the deuterium cross section (per nucleon)

$$\left(M^2 \frac{d^2\sigma}{dM^2 dx_F} \right)_{x_1 \gg x_2} \approx \frac{1}{3} \frac{4\pi\alpha^2}{3M^2} \left\{ \frac{4u(x_1) + d(x_1)}{9} \right\} \left[\bar{d}(x_2) + \bar{u}(x_2) \right] \tag{1.11}$$

where we have again taken the large-x_F limit. Thus, the deuterium cross section is directly proportional to the sum of the light antiquarks $\bar{d}(x) + \bar{u}(x)$.

In this thesis we describe and report results on the absolute measurement of continuum dimuon production in 800-GeV pp and pd interactions. The doubly-differential ($M^3 d^2\sigma/dM dx_F$) and triply-differential ($Ed^3\sigma/dp^3$) cross sections have been measured over a large range in the mass ($4 \leq M \leq 16.85$ GeV), x_F ($-0.05 \leq x_F \leq 0.8$) and p_T ($0 \leq p_T \leq 7$ GeV) of the muon pair. These data represent the first such measurement of the pp cross sections over an extended range of kinematics, while the pd cross sections have been measured over a wider kinematic range with greater statistical precision than has previously been achieved.

Traditionally, the Drell-Yan process is discussed in the context of probing the light antiquark distributions in the proton. And indeed, that was the primary motivation of this experiment. But it is clear from equations 1.10 and 1.11 that dimuon production also provides sensitivity to the valence distributions. While the kinematic range covered by previous dimuon measurements [Mor 91] has been limited to regions where the valence quarks are well constrained by DIS measurements, the E866 data cover a much wider kinematic range. Our data probe the valence out to $x \sim 0.8$, which provides an important measurement of the large-x behavior of the valence quarks complimentary to existing DIS measurements.